Advancing programmable metamaterials through machine learning-driven buckling strength optimization

Sangryun Lee [a,b], Junpyo Kwon [c,d], Hyunjun Kim [a], Robert O. Ritchie [a,c,d], Grace X. Gu [a,*]

[a] *Department of Mechanical Engineering, University of California, Berkeley, CA 94720, USA*
[b] *Department of Mechanical and Biomedical Engineering, Ewha Womans University, Seoul 03760, South Korea*
[c] *Materials Sciences Division Lawrence Berkeley National Laboratory, Berkeley, CA 94720, USA*
[d] *Department of Materials Science and Engineering, University of California, Berkeley, CA 94720, USA*

A B S T R A C T

Metamaterials are specially engineered materials distinguished by their unique properties not typically seen in naturally occurring materials. However, the challenge lies in achieving lightweight yet mechanically rigid architectures, as these properties are sometimes conflicting. For example, buckling strength is a critical property that needs to be enhanced since buckling can cause catastrophic failure of the lightweight metamaterials. In this study, we introduce a generative machine learning based approach to determine the superior geometries of metamaterials to maximize their buckling strength without compromising their elastic modulus. Our results, driven by machine learning based design, remarkably enhanced buckling strength (over 90 %) compared to conventional metamaterial designs. The simulation results are validated by a series of experimental testing and the mechanism of the high buckling strength is elucidated by correlating stress field with the metamaterial geometry. Our results provide insights into the interplay between shape and buckling strength, unveiling promising avenues for designing efficient metamaterials in future applications.

1. Introduction

Metamaterials are engineered materials with unique properties not typically seen in nature [1–8]. These properties are achieved by tuning the geometric structures of the material, rather than by altering its chemical composition. As a result, it is possible to achieve a wide range of properties by exploring the vast design space of metamaterial geometries [9,10]. Metamaterials are known for their lightweight and exceptional properties suitable for applications such as protective armor [11,12], sensors [13,14], and morphing airfoils [15,16]. The use of additive manufacturing techniques also allows for the fabrication of complex geometries, further increasing their potential applications [17–22].

Moreover, the inherent challenge arises from the fact that metamaterials typically incorporate voids and maintain a low relative density to achieve lightweight characteristics. However, this pursuit of reduced weight often comes at the expense of mechanical properties, rendering metamaterials more susceptible to unexpected buckling, particularly in their thin struts [23–25]. This buckling phenomenon can lead to a significant reduction in energy absorption capabilities due to the rapid

stress relaxation of the material [24]. Consequently, there is a growing body of literature in engineering metamaterials that exhibit enhanced resistance against buckling without significantly compromising their structural integrity. In addition, studies have been performed to exploit the post-buckling behavior of metamaterials to control the deformation modes of soft robotics or actuators [26,27]. For instance, Wang et al. has proposed soft machines driven by buckling actuators [28]. The buckling of soft material provides useful functions enabling actuators to deform through desired shapes. Therefore, programmable buckling behavior by tuning the metamaterials architecture can enable the design of metamaterials that can be selectively buckled at specific loads, enabling sophisticated control over deformation modes.

Achieving programmable buckling properties presents two challenges: determining the design variables critical for optimizing buckling strength and expanding design freedoms to allow for more versatile structural configurations. Studies have focused on the microstructure of metamaterials, incorporating the shape of the struts as a design variable for improving buckling strength [24,25,29,30]. However, only a few parameters have been considered due to the large computational cost for analyzing buckling behavior, which limits the design candidates for

optimization. Hence, the upper limit of buckling strength of meta-materials and the mechanism of shape-dependent buckling behavior have yet to be fully studied.

This study introduces a novel approach for optimizing the unit cell geometry of metamaterials to maximize their buckling strength without compromising their elastic modulus. The piecewise closed Bézier curve models a unit lattice of the metamaterials and allows a greater range of designs. Generative machine learning algorithm carries the optimization process and combines artificial neural networks and genetic optimization [31,32]. The neural networks allow for fast prediction [33–38] and speed up the optimization process by making informed decisions during genetic optimization. Additive manufacturing and compression testing verify the optimal metamaterial design for enhanced buckling strength and controllable post-buckling behavior. The results of this study provide insights into the relationship between shape and buckling strength and demonstrate a promising method for designing efficient meta-materials in the future.

2. Methods

2.1. Unit cell modeling and finite element analysis to predict buckling strength

In order to generate training datasets covering a large design space, a parametric curve described by a number of design variables is needed. In this study, a piecewise closed Bézier curve with a highly flexible design space describes a unit cell shape of metamaterials. The length of the unit cell is 1 cm. A total of 7 cubic Bézier curves are connected to make a quarter of the unit cell shape. First, 8 random points are created in the first quadrant of the unit cell, including one point on the x-axis and y-axis, respectively (Fig. 1(a)). Then, the angle between the x-axis and the line connecting each control point to the origin is calculated. After arranging the angles in ascending order, a cubic Bézier curve is created between two adjacent points. Two other control points between the two points are determined through the C^1 and C^2 continuity conditions for the adjacent Bézier curves. The metamaterial having periodic micro-structure is known to deform in the horizontal or out-of-plane direction as a post-buckling behavior. Therefore, this work adopts the symmetric

unit cell shape to the x and y axes to reduce the number of independent design variables and find the optimal shape with a reduced computational cost (Fig. 1(b)). The geometry of the unit cell is obtained through the x-axis, y-axis, and origin symmetry of the quarter geometry. The design variable is the coordinate of the independent control points that determines the unit cell's shape, i.e., 14 design parameters are used. 5 by 5 unit cells are used for a plate with a thickness of 3 mm (Fig. 1(c)) to consider infinitely periodic metamaterials. Previous work has shown the effect of the number of unit cells on the buckling strength [24]. When the metamaterial has a larger unit cells than 5 by 5, the metamaterial has a converged buckling strength, and the post-buckling behavior shows an insignificant difference compared to the larger system.

In this study, buckling analysis is performed using COMSOL multi-physics with the assumption of linear elastic buckling [39]. The linear hexahedron element is used for the buckling simulation of meta-materials. A rectangular mesh is generated on the frontal plane of the metamaterial, and then a sweep mesh is employed to construct the final three-dimensional mesh configuration. Approximately 56,000 elements are used for meshing the three-dimensional metamaterials. For boundary conditions, the bottom surface is fixed, and the displacement of 1 mm is applied to the top surface downward. Due to this boundary condition, the loadings applied on the top and bottom surfaces are symmetric, a feature that cannot be achieved using force boundary conditions. Therefore, the movement of the top surface is constrained horizontally to better align the computational condition with the experimental one. In our experiment, the top and bottom sides of the metamaterial are clamped by grips, inducing buckling as the top grips move in the vertical direction. Under this symmetric loading condition, we expect two buckling modes in our three-dimensional buckling simulations: (1) In-plane buckling and (2) Out-of-plane buckling. The buckling strength is calculated by multiplying the predicted eigenvalue by the average stress applied to the upper surface. By the assumption of linear elasticity, normalized Young's modulus $E_0 = 1$ (dimensionless) and a Poisson's ratio of $\nu = 0.25$, are used to generalize our results independent of material properties.
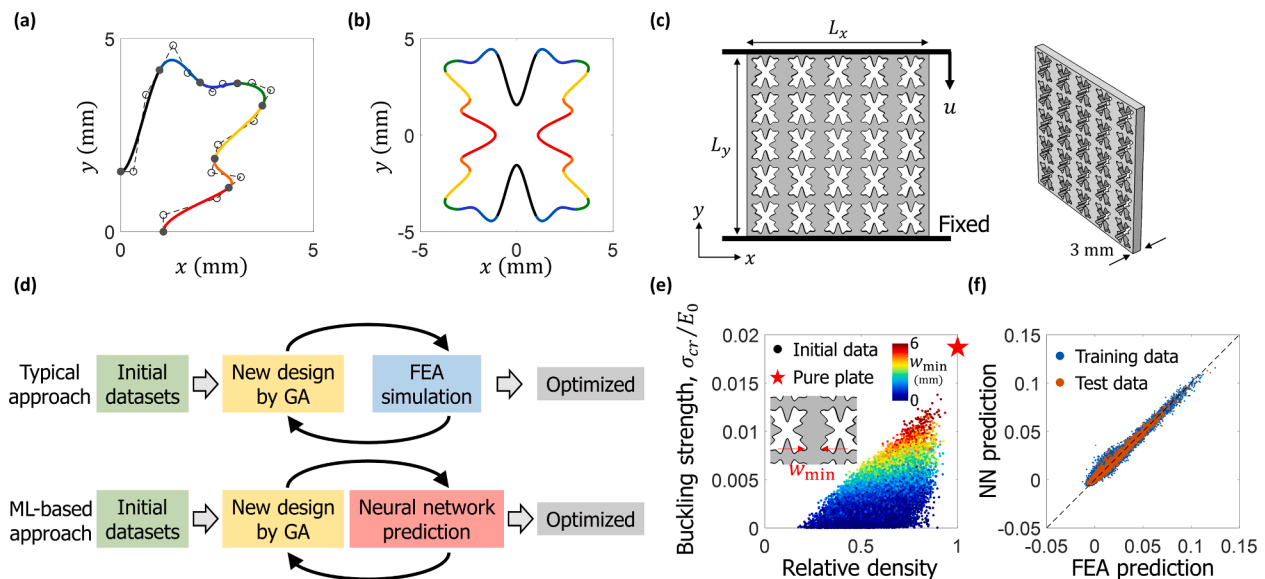

Fig. 1. (a) Piecewise Bézier curve in the first quadrant of the unit cell. Each color corresponds to a cubic Bézier curve. (b) A closed Bézier curve encompassing the unit cell. (c) Metamaterial modeled by the closed Bézier curve. The geometric dimensions L_x and L_y are both set at 50 mm. The bottom surface is fixed while a prescribed displacement u is applied along the negative y direction to apply compressive loading. The thickness of the metamaterial is 3 mm. (d) The flowchart outlining the two design optimization approaches. (e) Normalized buckling strength derived from 20,000 initial datasets. The buckling strength is normalized by the Young's modulus of the base material. The color represents the minimum thickness of the column along its axis. (f) Comparison of objective function values, as predicted by a trained neural network, with the results of finite element simulations. The R^2 value is 97.5 %.

2.2. Generative machine learning approach for design optimization

This study employs an artificial neural network (NN) to comprehend the intricate relationship between geometry and buckling strength in metamaterials, aiming to accelerate design optimization. The metamaterial's shape is optimized using a generative machine learning approach, generating 20,000 Bézier curves with corresponding buckling strengths predicted through finite element analysis (FEA). An objective function, incorporating the relative density, buckling strength, and target density, guides the optimization process. The NN, with 13 hidden layers and 14 neurons each, utilizes batch normalization and ResNet architecture. The NN is trained for 100 epochs, and the trained NNs are combined with genetic optimization (GO) to expedite the optimization process. The study introduces active learning to improve NN prediction accuracy, and the iteration of the algorithm converges to maximize buckling strength (Fig. 1(d)). The method proves more efficient than traditional GO due to the NN's faster prediction capabilities. Details are described in the Supporting Information.

2.3. Experimental setup

A polyjet additive manufacturing technique (Objet260 Connex3, Stratasys®) is used to fabricate our metamaterials with complex geometries. The fabrication process includes the utilization of an ultraviolet laser to cure the photopolymer layer-by-layer. The material called DM8530, which is a mixture of TangoBlackPlus and VeroWhite, was used as the base material for metamaterials [40]. The material DM8530 exhibits a Young's modulus of approximately 545 MPa, which is more than 180 times higher than that of pure TangoBlackPlus. This significantly higher stiffness compared to pure TangoBlackPlus makes DM8530 suitable for linear buckling experiments, as it demonstrates negligible nonlinear behavior prior to yielding [41]. To mimic the loading conditions applied to the upper and lower surfaces, pure plates with a length of 3 cm are extended from both the top and bottom surfaces, subsequently secured by a mechanical gripper. The experiment controls the compressive displacement of the grippers. Under the quasi-static loading condition, the loading rate is fixed at 5 mm/min with a strain rate of 1.6×10^{-3}/s. Buckling strength was determined as the
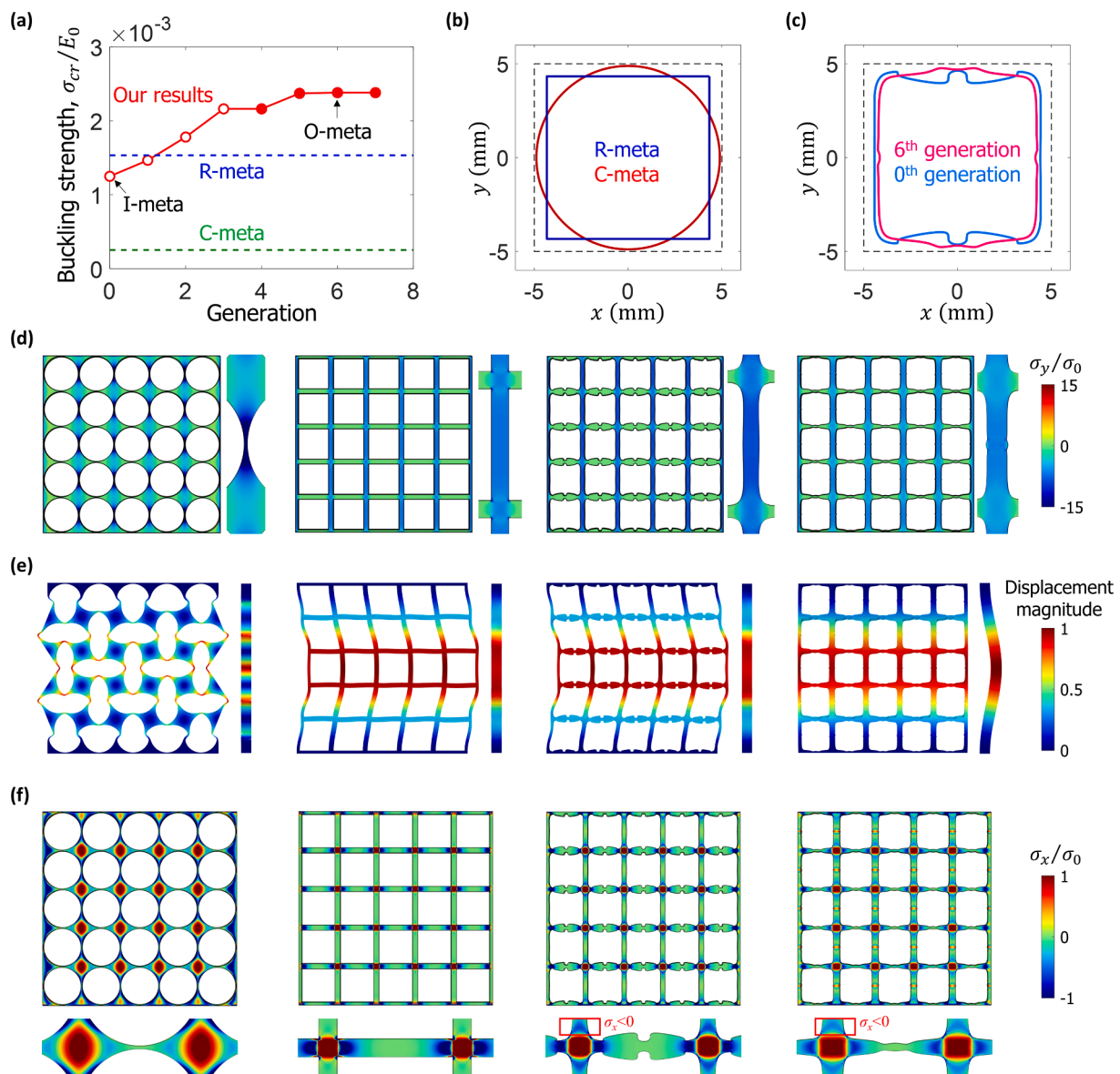

Fig. 2. (a) Normalized buckling strength of metamaterials during the optimization process. Each data point represents the maximum strength achieved within a given generation, with the 0th generation corresponding to the initial dataset. The filled mark implies out-of-plane post buckling behavior. (b)-(c) The unit cell shape of each metamaterial. The stress field ((d): σ_y, (f): σ_x) of the metamaterial under compressive loading in the y direction. (e) The first buckling mode shapes.

peak value along the achieved stress–strain curve.

3. Results and discussion

The initial datasets are prepared by generating random numbers for the coordinates of the control points. Fig. 1(e) shows the normalized buckling strength of our 20,000 initial datasets respect to their relative density. According to linear elasticity, the buckling strength is sensitive to the thickness of the column. Therefore, the minimum thickness of the column along its axis is calculated as the geometry feature of the metamaterial, and each mark in Fig. 1(e) is painted according to its minimum thickness value. As shown in the figure, the buckling strength increases with the minimum thickness, as expected. Compared with the pure plate cases, all the initial datasets have lower buckling strength due to the voids embedded in the metamaterial unit cell. The NN is trained with the initial design of the unit cell as input and the objective function value as the output. The NN prediction accuracy is validated by comparing the NN prediction against FEA (ground truth). The R^2 value is obtained by fitting our datasets into $y = x$ curve and the R^2 of the initial datasets is higher than 0.97, which implies high prediction accuracy (Fig. 1(f)).

The generative machine learning-based optimization approach is performed for the metamaterials with three relative densities including 25 %, 50 %, and 75 %. With a relative density of 25 %, the buckling strength increases as the optimization progresses, converging after the 5th generation (Fig. 2(a)). Because the buckling strength of the best design among 7th-generation datasets is lower than that of the 6th-generation, the best design of the 6th-generation datasets is considered the optimized design in this study. For the comparison of the optimized structure (O-meta) buckling strength, the study chose three reference metamaterial models: rectangular (R-meta), circular (C-meta), and best of initial datasets (I-meta). Compared to the other shapes, the unit cell of C-meta has a thin vertical column, resulting in high compressive stress and therefore the lowest buckling strength (Fig. 2(b) and (c)). The R-meta has 506 % and 23 % higher buckling strength compared to the C-meta and I-meta, respectively, and the O-meta has 55 % higher buckling strength than the R-meta. Hence, the O-meta has 842 %, 55 %, and 90 % enhanced buckling strength than C-meta, R-meta and I-meta, respectively.

The O-meta has a thicker column with a minimum thickness of around 1.5 mm compared to the reference models (1.3 mm, 0.2 mm, and 1.2 mm for R-meta, C-meta, and I-meta, respectively), and therefore low compressive stress is applied to the column under the same applied loading condition, resulting in the highest buckling strength (Fig. 2(d)). Previous simulations from the literature have shown that an optimal column shape with radius variation in the vertical column has uniform strain energy in buckling mode [42,43]. However, the variation of our optimized shape is small, since the relative density of 25 % is not high enough to have a sufficiently thick column. The FEA simulation in Fig. 2 (e) predicted the post-buckling patterns. In-plane buckling is observed in C-meta, R-meta, and I-meta, whereas out-of-plane buckling occurred in O-meta. Considering a pure plate subjected to a compressive load, it has two possible buckling modes: in-plane buckling mode and out-of-plane buckling mode. The buckling strength (σ_{cr}) and critical buckling load (P_{cr}) of the plate is determined by the Euler buckling theory, as shown in Equation (1):

$$\sigma_{\mathrm{cr}} = \frac{P_{cr}}{A} = \left(\frac{\pi}{L_e}\right)^2 \bullet \frac{E}{A} \bullet \left(\min(I_x, I_z)\right), \tag{1}$$

where A is the cross-sectional area of the plate, I is the planar second moments of area, E is the Young's modulus of the material and L_e is the effective length considering the length factor raised by the boundary conditions. Given the microstructure, boundary conditions, and material properties, the first post-buckling mode is determined by a competition between I_x and I_z. That is, in the case of a rectangular plate with width b

$= L_x$ and thickness t, the buckling strength and corresponding post-buckling mode are determined through a comparison of $I_x = (1/12)bt^3$ and $I_z = (1/12)tb^3$ values. When $b \gg t$, out-of-plane is the first mode with a low eigenvalue for buckling, and in-plane buckling is the second buckling mode with higher buckling strength. However, in the case of a metamaterial with low relative density, various in-plane deformation modes have been observed due to the thin columns. Thus, in-plane buckling becomes the first mode, and out-of-plane mode becomes the second mode for the metamaterial with a low relative density. Since the pure plate has the maximum buckling strength of metamaterial, to increase the buckling load of metamaterials at low relative density, the optimization proceeds to transition in the dominant buckling mode from in-plane to out-of-plane deformation.

The transition of the buckling mode is observed in accordance with the O-meta during the optimization process (Fig. 2(a)). From the 4th generation, the metamaterials with the best performance in each generation show out-of-plane buckling. Each buckling mode is predicted by the eigenvalue problem and the eigenvalue is calculated through the FEA buckling analysis. The eigenvalue is the ratio of the buckling strength and applied stress, *i.e.*, $\sigma_{cr}/\sigma_{applied}$, also known as the buckling load factor. As studied in the previous literature, the eigenvalues of the first and second modes converge to each other when the column has an optimized shape (radius variation) [42,43]. In this work, the eigenvalue of 1st and 2nd buckling mode is calculated by FEA. The best design among initial datasets has 1st eigenvalue of 0.398 and 2nd eigenvalue of 0.4528, showing the difference of 0.0546. The difference decreases as the optimization proceeds and eventually it is 0.0083 which means that the buckling strength of the two buckling modes become similar, as summarized in Supporting Information Table S1.

A comparison of σ_x explains the two different buckling modes of the metamaterials with low relative density. Under uniaxial compression loading in a downward direction ($-y$), the I-meta and O-meta have a compressive stress σ_x near the joint part where the vertical and horizontal beams intersect. When a compressive stress is applied to the lateral side of the column, buckling is prevented from occurring because the compressive stress suppresses the bending deformation, accompanying high buckling strength. The O-meta, with a larger compressive stress zone area, therefore results in higher buckling strength compared to R-meta. In a summary of our simulation results, the O-meta has the highest buckling strength because it has a thick vertical beam and large negative stress zone, which effectively reduces the slenderness of the column, compared to the other reference models.

Specimens are fabricated by 3D printing for the four cases to verify our optimization results, and three specimens are prepared for each case (Fig. 3(a)). The experiment uses a total of 12 specimens. As a result, the optimal shape has the highest buckling strength and stiffness showing a good agreement with the simulation results (Fig. 3(b) and (c)). The two deformation modes of the beam elements determine the stiffness. When their deformation predominantly involves stretching, the resultant stiffness is inherently higher compared to cases where bending dominates due to the nature of a higher axial stiffness than bending stiffness [32]. The optimization increases the cross-sectional area of the vertical column to improve the buckling strength; the effective stiffness is also improved because more materials are shifted toward the loading direction than in other cases. Furthermore, the optimized specimen showed an out-of-plane post-buckling mode whereas the rest showed in-plane buckling, which is also consistent with the post-buckling pattern predicted by the simulation (Fig. 3(d) and the compression testing video of four specimens shown in the Supporting Information as Video S1.

We optimized the buckling strength of the metamaterial with a high density of 50 % and 75 % using the generative design optimization approach (Fig. 4(a)). The column of O-meta with a density of 50 % is thicker compared to the horizontal beam, which is consistent with the case of 25 % relative density. In addition, due to the sufficiently high density, it has a larger variation compared to the 25 % density, and the shape of the column is very similar to the optimal shape of the column
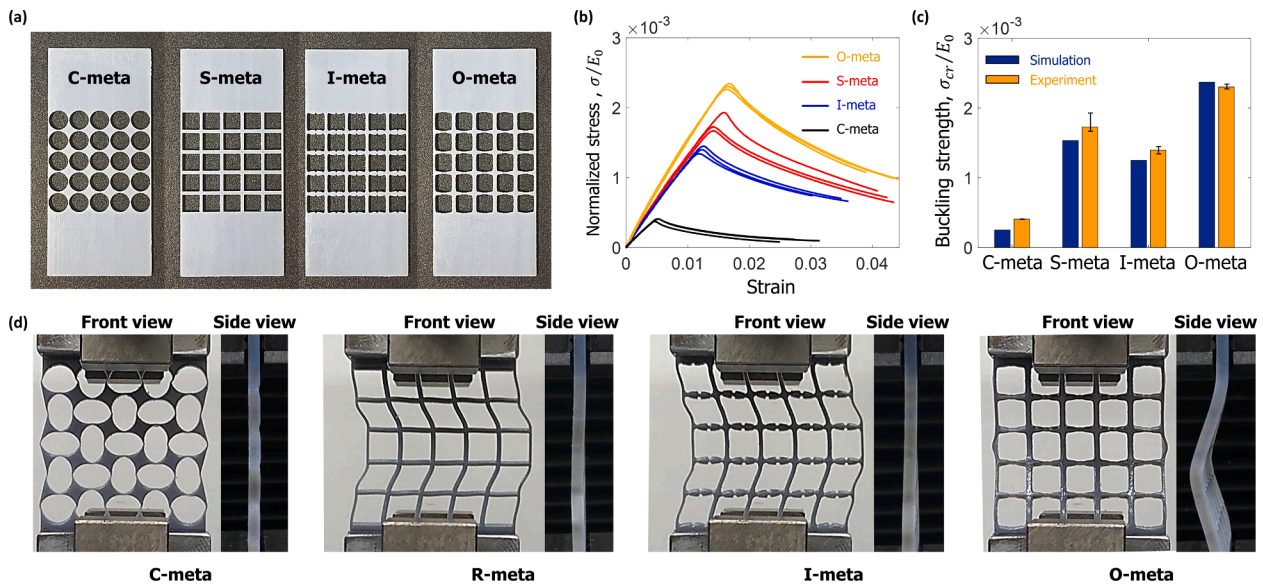
Fig. 3. (a) The fabricated specimens for compression testing. (b) Stress–strain curves of the four specimens ($n = 3$ samples for each microstructure). Stress values are normalized by the Young's modulus of the base material, and the length of the error bar represents the difference between the maximum and minimum values of the three samples. (c) Normalized buckling strength of each specimen. (d) The captured deformation configuration observed in each sample subsequent to the initiation of buckling.
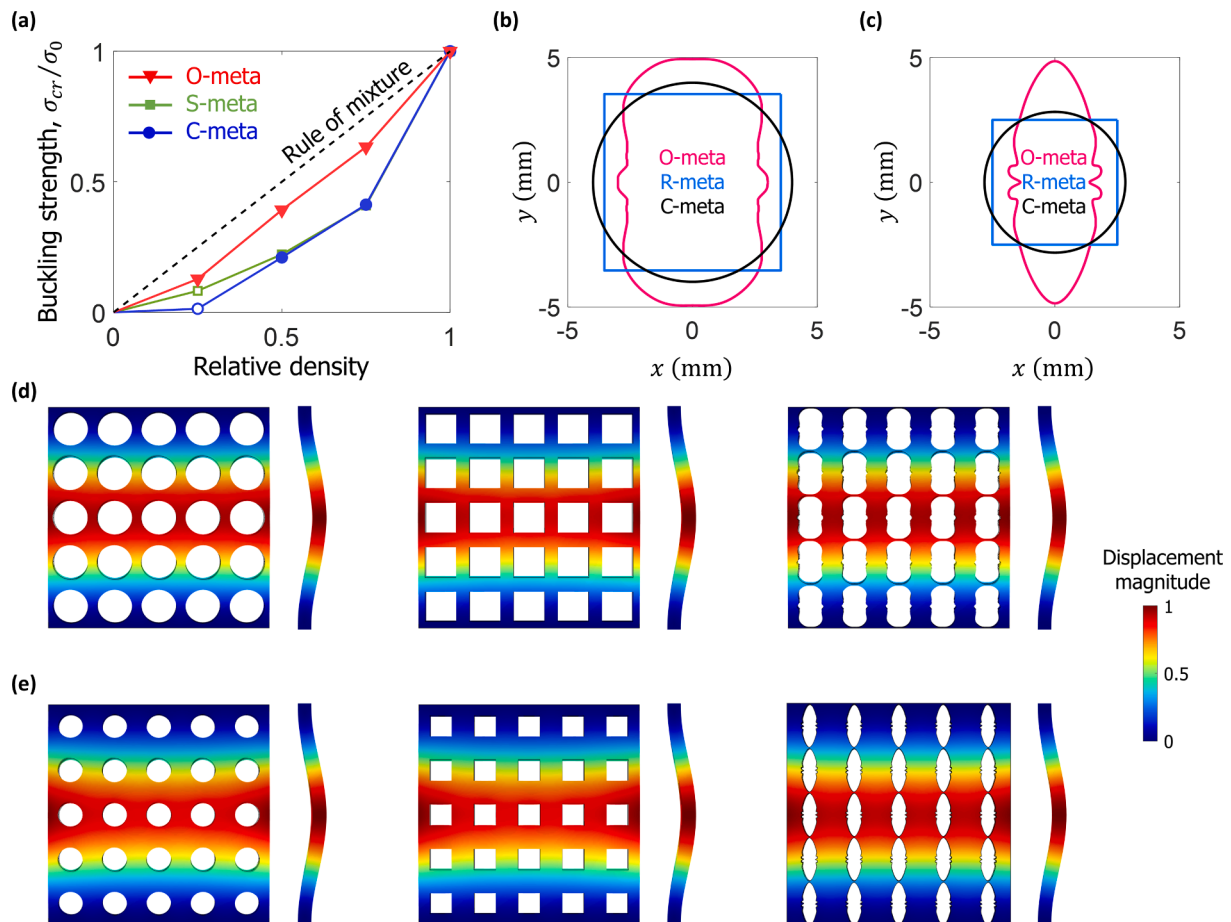

Fig. 4. (a) Buckling strength with respect to different relative densities of the metamaterial. The shape of the unit cell corresponding to a relative density of (b) 50 % and (c) 75 %. The first buckling mode shape for the case of (d) 50 % and (e) 75 % relative density.

proposed in a previous study [44]. In particular, the relative density of 75 % case has more waviness than 50 %, which has a more complex shape for more efficient stress distribution. Interestingly, the horizontal beam of all O-meta is very thin, and it is believed that the thickness of the beam does not significantly affect the buckling strength and post-buckling behavior. However, the thickness is essential for the high buckling strength due to the suppression of deformation in the lateral direction (Fig. 4(b) and (c)). Hence, the horizontal beam is essential to increase the buckling strength. But the beam does not need to be thick as it benefits from generating thicker columns while maintaining the thin thickness of the horizontal beam.

Given the optimized microstructure, we further optimize the buckling strength by modeling the shape of the unit cell as a rounded rectangle with its width w and height h consisting of elliptic corners having a, and b as semi-axis, respectively (Figure S2). We predict the buckling strength of the metamaterials with the same density in the range $h_0 - 1.7$ mm $< h < h_0 + 1.7$ mm, and $w_0 - 1$ mm $< w < w_0 + 1$ mm, where $w_0 = 5.5$ mm and $h_0 = 9.25$ mm are approximated value from our optimized shape. Within these ranges, about 1000 different rounded rectangle unit cells are generated under a fixed relative density of 0.5, with the buckling strength compared with that of our optimized shape. As a result, the best-simplified metamaterial has a slightly higher normalized buckling strength (0.3979) compared to that of the optimal shape (0.3921); however, the improvement is insignificant, implying that O-meta is close to the optimum structure. One of the possible reasons why our generative design approach could not generate the rounded rectangle unit cell is because it is difficult to generate the round rectangle using our composite Bézier curves. The column of the unit cell consists of 2 to 4 cubic Bézier curve and the smoothness of the column is very sensitive to the coordinate of the control point on the *x*-axis since it is quite difficult to obtain parabola shape using two jointed cubic curves. Therefore, in order to obtain the rounded rectangle model using our composite cubic Bézier curve, the control points in the Bézier curves of column part must be controlled very carefully.

The relative strength-density results for the three geometries are plotted using the Gibson Ashby plot that is widely used for cellular structures, as shown in Fig. 4(a). O-meta has higher buckling strength than two typical unit cells for the entire range of relative density. The difference between the strength of R-meta and C-meta becomes negligible as the density increases since the two shapes are similar at cases of high relative density. The O-meta shows out-of-plane post-buckling behavior for all relative density cases whereas the two other metamaterials show in-plane buckling behavior at low density and out-of-plane buckling behavior at high density.

This work demonstrates controllable buckling behavior and enhanced buckling strength at low relative density. However, our analysis assumes linear elasticity, thereby excluding the consideration of geometric nonlinearity and self-contact, which are commonly observed in soft materials. Future investigations could focus on controlling buckling behavior under large deformations to uncover additional local buckling mechanisms triggered by geometric nonlinearity, such as crease localization, fold localization, and ridge location [45].

4. Conclusions

We enhance the buckling strength of metamaterials via a generative machine learning-based design optimization approach. The closed piecewise Bézier curve is employed to model the shape of the metamaterial with more flexible design space than other models. The NN is trained to predict objective function consisting of a penalty term of relative density and buckling strength using the shape of the unit cell as an input. The NN is then combined with genetic optimization and used to make greedy decisions during optimization, which accelerates the optimization process. The optimized structure has improved buckling strength by 842 %, 55 %, and 90 % compared with three reference models and shows predominant post-buckling behavior compared to

these three models. The metamaterials are fabricated by additive manufacturing and our design is validated by compressive testing. The buckling strength measured from our experiments is matched with simulation results. We believe this innovative approach opens up possibilities for advancing mechanical properties beyond the constraints of human knowledge in metamaterial design.

Declaration of competing interest

The authors declare that they have no known competing financial interests or personal relationships that could have appeared to influence the work reported in this paper.

Data availability

All data supporting this study are included in the article and/or supporting information.

Appendix A. Supplementary material

Supplementary data to this article can be found online at https://doi.org/10.1016/j.cossms.2024.101161.

References

[1] D. Schurig, J.J. Mock, B.J. Justice, S.A. Cummer, J.B. Pendry, A.F. Starr, D. R. Smith, Metamaterial electromagnetic cloak at microwave frequencies, Science 314 (5801) (2006) 977–980.

[2] K.H. Matlack, M. Serra-Garcia, A. Palermo, S.D. Huber, C. Daraio, Designing perturbative metamaterials from discrete models, Nat. Mater. 17 (4) (2018) 323–328.

[3] T.A. Schaedler, A.J. Jacobsen, A. Torrents, A.E. Sorensen, J. Lian, J.R. Greer, L. Valdevit, W.B. Carter, Ultralight metallic microlattices, Science 334 (6058) (2011) 962–965.

[4] Q.M. Wang, J.A. Jackson, Q. Ge, J.B. Hopkins, C.M. Spadaccini, N.X. Fang, Lightweight mechanical metamaterials with tunable negative thermal expansion, Phys. Rev. Lett. 117 (17) (2016).

[5] J.K. Wilt, C. Yang, G.X. Gu, Accelerating auxetic metamaterial design with deep learning, Adv. Eng. Mater. 22 (5) (2020) 1901266.

[6] K. Aas, M. Jullum, A. Løland, Explaining individual predictions when features are dependent: More accurate approximations to Shapley values, Artif. Intell. 298 (2021) 103502.

[7] O.R. Bilal, A. Foehr, C. Daraio, Bistable metamaterial for switching and cascading elastic vibrations, Proc. Natl. Acad. Sci. 114 (18) (2017) 4603–4606.

[8] S. Hajarolasvadi, A.E. Elbanna, Dynamics of metamaterial beams consisting of periodically-coupled parallel flexural elements: A theoretical study, J. Phys. D Appl. Phys. 52 (31) (2019) 315101.

[9] J. Plocher, A. Panesar, Review on design and structural optimisation in additive manufacturing: Towards next-generation lightweight structures, Mater Design 183 (2019).

[10] L.E. Murr, S.M. Gaytan, D.A. Ramirez, E. Martinez, J. Hernandez, K.N. Amato, P. W. Shindo, F.R. Medina, R.B. Wicker, Metal fabrication by additive manufacturing using laser and electron beam melting technologies, J. Mater. Sci. Technol. 28 (1) (2012) 1–14.

[11] C.M. Portela, B.W. Edwards, D. Veysset, Y.C. Sun, K.A. Nelson, D.M. Kochmann, J. R. Greer, Supersonic impact resilience of nanoarchitected carbon, Nat. Mater. 20 (11) (2021), 1491-+.

[12] S.Y. Jeon, B.J. Shen, N.A. Traugutt, Z.Y. Zhu, L.C. Fang, C.M. Yakacki, T. D. Nguyen, S.H. Kang, Synergistic energy absorption mechanisms of architected liquid crystal elastomers, Adv. Mater. 34 (14) (2022).

[13] Y.I. Abdulkarim, L.W. Deng, H. Luo, S.X. Huang, M. Karaaslan, O. Altintas, M. Bakir, F.F. Muhammadsharif, H.N. Awl, C. Sabah, K.S.L. Al-badri, Design and study of a metamaterial based sensor for the application of liquid chemicals detection (vol 9, pg 10291, J. Mater. Res. Technol. 11 (2021) (2020) 1111.

[14] M.R. Islam, M.T. Islam, M.M. Salaheldeen, B. Bais, S.H.A. Almalki, H. Alsaif, M. S. Islam, Metamaterial sensor based on rectangular enclosed adjacent triple circle

split ring resonator with good quality factor for microwave sensing application, Sci. Rep.-Uk 12 (1) (2022).

[15] P. Bettini, A. Airoldi, G. Sala, L. Di Landro, M. Ruzzene, A. Spadoni, Composite chiral structures for morphing airfoils: Numerical analyses and development of a manufacturing process, Compos. Part B-Eng. 41 (2) (2010) 133–147.

[16] A. Airoldi, P. Bettini, P. Panichelli, M.F. Oktem, G. Sala, Chiral topologies for composite morphing structures - Part I: Development of a chiral rib for deformable airfoils, Phys. Status Solidi B 252 (7) (2015) 1435–1445.

[17] G.X. Gu, M. Takaffoli, M.J. Buehler, Hierarchically enhanced impact resistance of bioinspired composites, Adv. Mater. 29 (28) (2017).

[18] S.L. Lu, M. Qian, H.P. Tang, M. Yan, J. Wang, D.H. StJohn, Massive transformation in Ti-6Al-4V additively manufactured by selective electron beam melting, Acta Mater. 104 (2016) 303–311.

[19] S.C.-y. Shen, M.J. Buehler, Nature-inspired architected materials using unsupervised deep learning, Commun. Eng. 1 (1) (2022) 37.

[20] G. Campoli, M.S. Borleffs, S.A. Yavari, R. Wauthle, H. Weinans, A.A. Zadpoor, Mechanical properties of open-cell metallic biomaterials manufactured using additive manufacturing, Mater Design 49 (2013) 957–965.

[21] A. Ghimire, Y.-Y. Tsai, P.-Y. Chen, S.-W. Chang, Tunable interface hardening: Designing tough bio-inspired composites through 3D printing, testing, and computational validation, Compos. B Eng. 215 (2021) 108754.

[22] Z. Jin, Z. Zhang, K. Demir, G.X. Gu, Machine learning for advanced additive manufacturing, Matter 3 (5) (2020) 1541–1556.

[23] Y.H. He, Y. Zhou, Z.S. Liu, K.M. Liew, Buckling and pattern transformation of modified periodic lattice structures, Extreme Mech. Lett. 22 (2018) 112–121.

[24] Y.J. Wang, Z.Y. Chi, J.X. Liu, On buckling behaviors of a typical bending-dominated periodic lattice, Compos. Struct. 258 (2021).

[25] H. Yang, L. Ma, Multi-stable mechanical metamaterials by elastic buckling instability, J. Mater. Sci. 54 (4) (2019) 3509–3526.

[26] Y.P. Song, R.M. Panas, S. Chizari, L.A. Shaw, J.A. Jackson, J.B. Hopkins, A. J. Pascall, Additively manufacturable micro-mechanical logic gates, Nat. Commun. 10 (2019).

[27] Y.J. Jiang, L.M. Korpas, J.R. Raney, Bifurcation-based embodied logic and autonomous actuation, Nat. Commun. 10 (2019).

[28] G.L. Wang, M.E. Li, J.X. Zhou, Modeling soft machines driven by buckling actuators, Int. J. Mech. Sci. 157 (2019) 662–667.

[29] J. Hua, H.S. Lei, C.F. Gao, X.G. Guo, D.N. Fang, Parameters analysis and optimization of a typical multistable mechanical metamaterial, Extreme Mech. Lett. 35 (2020).

[30] A. Jha, I. Dayyani, Shape optimisation and buckling analysis of large strain zero Poisson's ratio fish-cells metamaterial for morphing structures, Compos. Struct. 268 (2021).

[31] S. Lee, Z.Z. Zhang, G.X. Gu, Generative machine learning algorithm for lattice structures with superior mechanical properties, Mater. Horiz. 9 (3) (2022).

[32] S. Lee, Z. Zhang, G.X. Gu, Deep learning accelerated design of mechanically efficient architected materials, ACS Appl. Mater. Interfaces (2023).

[33] P. Reiser, M. Neubert, A. Eberhard, L. Torresi, C. Zhou, C. Shao, H. Metni, C. van Hoesel, H. Schopmans, T. Sommer, Graph neural networks for materials science and chemistry, Commun. Mater. 3 (1) (2022) 93.

[34] Y. Kim, Y. Kim, C. Yang, K. Park, G.X. Gu, S. Ryu, Deep learning framework for material design space exploration using active transfer learning and data augmentation, npj Comput. Mater. 7 (1) (2021) 1–7.

[35] H. Liu, Z. Huang, S. Schoenholz, E.D. Cubuk, M.M. Smedskjaer, Y. Sun, W. Wang, M. Bauchy, Learning molecular dynamics: predicting the dynamics of glasses by a machine learning simulator, Mater. Horiz. (2023).

[36] B. Ni, D.L. Kaplan, M.J. Buehler, Generative design of de novo proteins based on secondary-structure constraints using an attention-based diffusion model, Chem (2023).

[37] S. Mohammadzadeh, E. Lejeune, Predicting mechanically driven full-field quantities of interest with deep learning-based metamodels, Extreme Mech. Lett. 50 (2022) 101566.

[38] Z. Zhang, Z. Jin, G.X. Gu, Efficient pneumatic actuation modeling using hybrid physics-based and data-driven framework, Cell Reports Physical Science 3 (4) (2022) 100842.

[39] S. COMSOL Multiphysics®. www.comsol.com. COMSOL AB, Sweden.

[40] A.Y. Lee, J. An, C.K. Chua, Y. Zhang, Preliminary investigation of the reversible 4D printing of a dual-layer component, Engineering-Prc 5 (6) (2019) 1159–1170.

[41] J.E.M. Teoh, J. An, X.F. Feng, Y. Zhao, C.K. Chua, Y. Liu, Design and 4D printing of cross-folded origami structures: a preliminary investigation, Materials 11 (3) (2018).

[42] W. Szyszkowski, L.G. Watson, Optimization of the buckling load of columns and frames, Eng. Struct. 10 (4) (1988) 249–256.

[43] D. Manickarajah, Y.M. Xie, G.P. Steven, Optimisation of columns and frames against buckling, Comput. Struct. 75 (1) (2000) 45–54.

[44] I. Tadjbakhsh, J.B. Keller, Strongest Columns and Isoperimetric Inequalities for Eigenvalues, J. Appl. Mech. 29 (1) (1962) 159–164.

[45] M.Z. Diab, T. Zhang, R.K. Zhao, H.J. Gao, K.S. Kim, mechanics of creasing: from instantaneous to setback creases, P. Roy. Soc. a-Math. Phy. 469 (2157) (2013).